

## Article

# Assessment of the Rainfall Trend Effect on Meteorological and Hydrological Drought in the Upper Sebou Basin, Morocco

Ridouane Kessabi <sup>1</sup>, Mohamed Hanchane <sup>1</sup>, Nir Y. Krakauer <sup>2,\*</sup> and Mohamed Belmahi <sup>3</sup>

<sup>1</sup> Department of Geography FLSH Dhar el Mehraz, Mohamed Ben Abdellah University Fez, Fes 30000, Morocco; ridouane.kessabi@usmba.ac.ma (R.K.); mohamed.hanchane@usmba.ac.ma (M.H.)

<sup>2</sup> Department of Civil Engineering and NOAA-CESSRST, The City College of New York, New York, NY 10031, USA

<sup>3</sup> Ecole Normale Supérieure de Rabat, Mohammed V University, Rabat 5118, Morocco

\* Correspondence: nkrakauer@ccny.cuny.edu

## Abstract

The upper Sebou River occupies a strategic territory draining varied mountain reaches in northern Morocco. As such, it is rich in surface water resources and karst springs with important downstream uses. However, the variability of rainfall threatens its water potential, making it highly vulnerable and at risk of desiccation. This study explores rainfall trends and their effects on streamflow and water resource availability. Data from three stations representing the upstream section of the watershed, along with two streamflow series—one for the upper Sebou River (Pont Medz) and the other for the Ain Timdrine karst spring—cover the period from 1956 to 2018. The methodology employs Mann–Kendall trend tests, Sen’s Slope test, and the Standardized Precipitation Index (SPI) for rainfall series, as well as the Streamflow Drought Index (SDI) for hydrological series. The results demonstrate a decline in rainfall since 1979, significant at the 5% threshold. This trend has an immediate impact on the flow rates of the area’s rivers and karst springs, which have also tended to decline, with a succession of dry years and seasons since 1980. This observation highlights the depletion of water resources of the fragile upper Sebou region in the face of decreasing rainfall and snowfall, compounded by the rampant and unsustainable exploitation of groundwater resources linked to the development of irrigated cash crops in the Middle Atlas Mountains.

**Keywords:** rainfall; SPI; water resources; SDI; upper Sebou

## 1. Introduction

Morocco has been experiencing a severe drought for seven consecutive years, with a sharp decline in rainfall during the rainy season. This decline in rainfall began more than 40 years ago; various studies have identified the early 1980s as a turning point towards more arid and drier conditions, marked by a succession of years with rainfall deficits [1–6]. This situation has caused unprecedented pressure on surface water resources and especially groundwater reserves. The various aquifers have experienced intense exploitation and advanced depletion [7–9]. This decline in rainfall is accompanied by a rise in minimum and maximum temperatures [10–13]. This increase further reinforces atmospheric demand through extreme evapotranspiration [14], especially during the rather long summer dry season, which lasts six months or even longer in some areas.

Drought is the most dangerous natural hazard threatening Morocco’s economy [15], given the importance of the agricultural sector in employment, accounting for nearly 40% of



Academic Editor: Charles Jones

Received: 7 April 2026

Revised: 22 May 2026

Accepted: 24 May 2026

Published: 1 June 2026

**Copyright:** © 2026 by the authors.

Licensee MDPI, Basel, Switzerland.

This article is an open access article distributed under the terms and

conditions of the [Creative Commons Attribution \(CC BY\) license](https://creativecommons.org/licenses/by/4.0/).

the workforce and, in the overall structure of the country's economy, 18% of the gross domestic product (GDP) [16–18]. This hazard even threatens the political stability of the state through various protests against the failure of public policies in the area of drinking water supply, especially for rural communities [19–22]. The threat also extends to the population's food security, with soaring food prices being recorded and denounced by social movements [23]. Future projections indicate an increase in drought events, necessitating a rapid response to adapt to the new situation [24]. This alarming observation has not prompted public authorities to revise agricultural policies, which are partly responsible for promoting irrational irrigation of cash crops for export purposes and to enrich the political elites themselves [25].

The Mediterranean region, which shares climatic and geographic similarities and in whose western margin Morocco is located, has experienced increasing drought frequency and severity due to precipitation variability, adversely affecting water resources. Future projections indicate more intense hydrological droughts, particularly in developing countries along the southern and eastern Mediterranean coasts [26], as also confirmed by [27–29].

The study of drought remains somewhat complex given the irregular nature of this phenomenon [30]. Scientists have developed several indices and methods to quantify this potentially fatal risk [31–33]. Climatic or meteorological drought is defined as a rainfall deficit over a given period, generally a month, several months, a season, or a year, and in a given location, compared to the average observed over a long period for these time scales [34,35]. The accumulation of climatic drought over months and seasons leads to hydrological drought, with a decrease in water levels in dams, lakes, rivers, and even a drop in groundwater [36]. The transition from meteorological drought to hydrological drought is difficult to quantify.

Among the meteorological drought indices developed by the scientific community is the Standardized Precipitation Index (SPI). The robustness of this index and its use in different climatic zones worldwide give it a considerable advantage. Based solely on precipitation as a climatic variable, it is simple to calculate and can be used across multiple time scales [37]. Other indices have attempted to improve upon its capabilities, such as the Standardized Precipitation Evapotranspiration Index (SPEI), by incorporating temperature and evaporation factors, given the effect of these elements on drought intensification [38]. To study hydrological drought, indices such as the Standardized Runoff Index (SRI), calculated using the same methods as the SPI [39,40], and the Streamflow Drought Index (SDI), proposed by [41,42], are available. The SDI is widely used to study streamflow drought, and the study by [43] in Iran demonstrates its ability to characterize the phenomenon across multiple time scales. In Africa, the work of [44] uses the SDI to describe the effect of drought on streamflow in Ethiopia. The study by [45] uses the same method to explore the dryness of flows in Turkey. In Morocco, specifically in the Innaoun basin, near the upper Sebou River, the study by [46] used the SPI and SDI indices to investigate climatic and hydrological drought. The study [47] in the Tansift basin uses SPI indices combined with normalized difference vegetation index (NDVI) and piezometric data to study drought. In the Tafilalt region, the study by [48] utilizes the SPI and SPEI indices in addition to the Standardized Groundwater Index (SGI); their results reveal dire projections and serious threats to the water resources of a region already experiencing desertification. The study by [32] explores drought using SPI and trend tests in the Tansift area. Also in Oum Er-bia basin, the work of [49] demonstrated the extent of the drought in recent years using indices combining rainfall, groundwater, and surface water. All of these studies highlight the fragility of water resources, which are subject to unsustainable exploitation, with groundwater being overexploited through inappropriate agricultural practices.

The aim of this study is to explore the long-term links between rainfall, meteorological drought, and hydrological drought in the upper Sebou Basin. The SPI and SDI indices were used to standardize hydroclimatic data series at three rainfall stations and two hydrological series: one for surface streamflow (Pont Medz) and another for a karst spring (Ain Timdrine), which more accurately characterizes complex and slow hydrogeological flows. This choice is based on the logic of diversifying the hydroclimatic series to understand the behavior of the different systems and to accurately quantify the relationships between them. Trend and break tests in the hydroclimatic series are performed using the Mann–Kendall test; the sequential Mann–Kendall test, SQMK; the Sen Slope; and the Pettitt test. This document is organized as follows: (1) a presentation of the data, the study area, and the methods used; (2) the results are presented for the rainfall series, followed by a presentation of the standardized rainfall and streamflow indices; (3) correlations between the different indices calculated for several time scales are also discussed; and (4) a discussion is developed at the end to compare our results with the scientific literature published on the subject in Morocco.

## 2. Materials and Methods

### 2.1. Study Area

The upper Sebou Basin forms the upstream part of the Sebou Basin, the richest in water in Morocco. This sub-basin is located between longitude 4° and 5.2° west and latitude 33° and 34° north Figure 1. It covers an area of 4450 km<sup>2</sup>, representing 11% of the Greater Sebou Basin. It primarily drains the folded Middle Atlas Mountains to the south and the western slopes of the Middle Atlas Mountains to the northeast. This sub-basin is composed of the following tributaries: the Guigou River, the Zeloul River, and the Ait Makhchoune River.

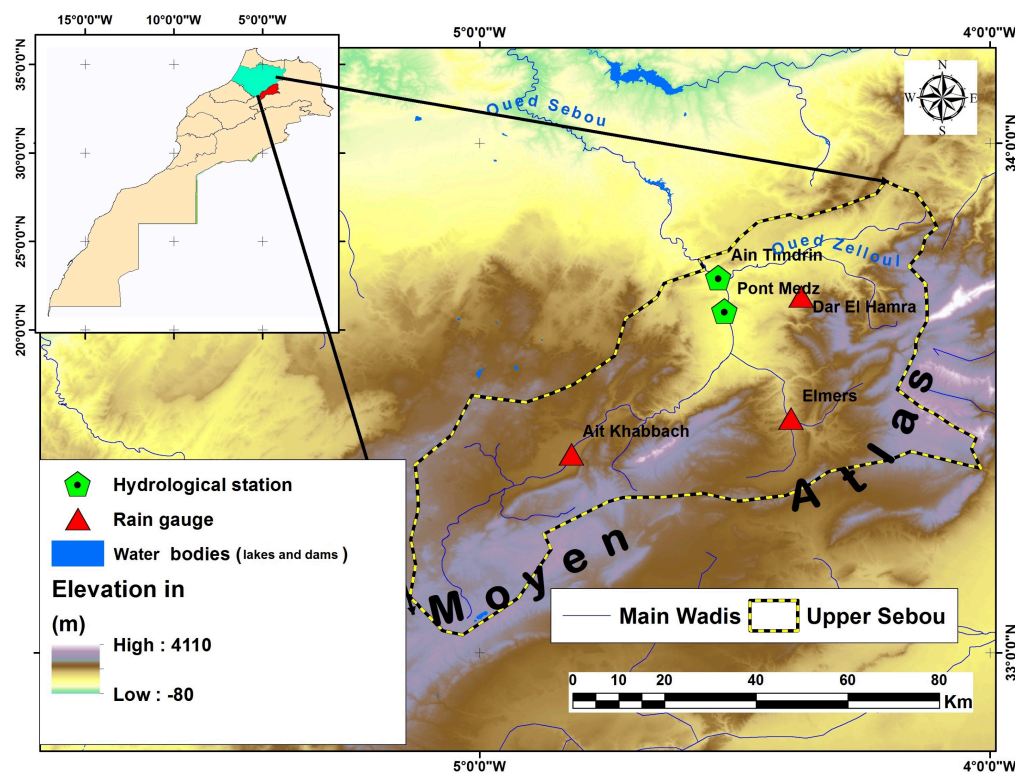


**Figure 1.** Location map of the upper Sebou Basin.

Elevations range from 213 m, the lowest point in the area (the northern part of the Sebou Valley), to 3171 m at the peaks of the Bouiblanc massif. The Sebou Valley, Mdaz, and Zeloul constitute the low-lying areas, while the Sefrou region and the Ribat El Khayer

plateaus form the intermediate zones leading to the high, folded mountain ranges such as the Bouiblane, Ich-Ntili, and Tichoukt massifs. The southwestern part of the Middle Atlas Mountains, on the other hand, is more flat and less rugged.

2.2. Data and Methods

The rainfall and hydrological data used for this study comes from the Sebou River Basin Water Agency (ABHS), the public authority responsible for monitoring and controlling all water-related activities in the basin. The selected three measurement stations are located upstream of the upper Sebou River to characterize the drought in the areas that supply the upper Sebou watershed. Table 1 presents the three rainfall stations and some basic statistics from their time series, which cover the period 1961–2019.

Table 1. Statistics of the rainfall series used.

ID	Station	Long°	Lat°	Elevation (masl)	Min (mm)	Max (mm)	Mean Annual (mm)	SD (mm)	CV%
S1	Ait Khabbach	−4.82	33.39	1491	180.5	684.4	378	111	29
S2	Dar El Hamra	−4.37	33.70	1142	221.1	894.9	495	144	29
S3	Elmers	−4.39	33.46	1242	205.2	832.5	454	139	31

To explore the effect of climate variability on water resources in springs and wadis (watercourses), two hydrological series were used: one for the Ain Timdrin spring (a karst spring) and the other for the Pont Medz station, which monitors the upstream flow of the upper Sebou River. While geographically very close to each other, from a hydrological point of view, they represent two completely different systems; Table 2 summarizes their basic statistics.

Table 2. Hydrological series statistics in m<sup>3</sup>/s.

ID	Station Name	Long	Lat.	Observation Period	Altitude (masl)	Min m <sup>3</sup> /s	Max m <sup>3</sup> /s	Mean m <sup>3</sup> /s	SD (m <sup>3</sup> /s)	CV%
H1	Ain Timdrin	−4.532	33.735	1956–2018	677	4.48	35.31	16.06	7.24	45%
H2	Pont Medz	−4.520	33.670	1957–2017	742	1.31	22.00	6.11	3.99	65%

2.3. Standardized Precipitation Index (SPI)

The SPI, widely used to explore drought based on rainfall data alone, was developed by [37] and described in detail by [38]. It measures rainfall anomalies at a given location by comparing the total rainfall amounts observed over an accumulation period (time scale) of interest (e.g., 1, 3, 12, 48 months) with the long-term rainfall history for that period.

The historical record is fitted to a probability distribution (typically the “gamma” distribution); then, it is transformed into a normal distribution so that the average SPI of the place considered and for the period of time studied is equal to zero.

The SPI is then calculated as follows:

$$g(x) = \frac{1}{\beta^\alpha \Gamma(\alpha)} x^{\alpha-1} e^{-\frac{x}{\beta}} \quad (x > 0)$$

With  $\Gamma(\alpha)$  being the Gamma function;  $x$  in (mm) being the amount of precipitation ( $x > 0$ );  $\alpha$  being the shape parameter ( $\alpha > 0$ ); and  $\beta$  being the scale parameter ( $\beta > 0$ ). For more information see [38].

This work focuses on drought events, neglecting the wet phases in the rainfall series, which are characterized by positive SPI and SDI (Table 3).

**Table 3.** Classification of negative SPI and SDI anomalies (McKee et al., 1995) [38].

Drought Class	SPI Class	Description	SDI Criterion
Slightly dry, near normal	−0.5 to −0.99	Mild drought	$-1.0 \leq \text{SDI} < 0.0$
Moderately dry	−1 to −1.49	Moderate drought	$-1.5 \leq \text{SDI} < -1.0$
Severely dry	−1.5 to −1.99	Severe drought	$-2 \leq \text{SDI} < -1.5$
Extremely dry	−2 and less	Extreme drought	$\text{SDI} < -2$

2.4. Streamflow Drought (SDI)

Referring to the work of [41], if a time series of monthly flows  $Q_{i,j}$  is available, in which  $i$  denotes the hydrological year and  $j$  the month of that hydrological year ( $j = 1$  for October and  $j = 12$  for September),  $V_{i,k}$  can be obtained from the following equation:

$$V_{i,k} = \sum_{j=1}^{3k} Q_{i,j} \quad i = 1, 2, \dots \quad j = 1, 2, \dots, 12k = 1, 2, 3, 4$$

in which  $V_{i,k}$  is the cumulative flow volume for the  $i$ -th hydrological year and the  $k$ -th reference period,  $k = 1$  for October–December,  $k = 2$  for October–March,  $k = 3$  for October–June, and  $k = 4$  for October–September.

Based on the cumulative flow volumes  $V_{i,k}$ , the Streamflow Drought Index (SDI) is defined for each reference period  $k$  of the  $i$ -th hydrological year as follows:

$$SDI_{i,k} = \frac{V_{i,k} - \bar{V}_k}{s_k} \quad i = 1, 2, \dots, k = 1, 2, 3, 4$$

where  $V_{i,k}$  is the cumulative streamflow volume for the  $i$ th period in the  $k$ -month reference interval, the  $\bar{V}_k$  is the long-term mean cumulative streamflow for the  $k$ -month interval, and  $s_k$  is the standard deviation of cumulative streamflow for the  $k$ -month interval.

We calculated the SPI at 12-month and 3-month time scales. The 12-month scale (SPI12) reflects the effects of precipitation deficits on hydrological drought, whereas the 3-month scale (SPI3) is used to monitor meteorological drought and its relationship with surface runoff. SPI12 is based on a single annual value, while SPI3 is computed first for consecutive 3-month periods (e.g., September–October–November and December–January–February) for seasonal purposes and second in cumulative form for a long-term trend test. The SDI was calculated at annual, seasonal, and monthly time scales to enable correlations with SPI at both annual and seasonal scales.

A Pearson correlation matrix was generated using the R programming environment to analyze the relationships between the seasonal SPI and SDI values across all considered time series, highlighting the strength and significance of their correlations.

2.5. Trend and Break-Even Tests

(A) The Mann–Kendall Sequential Test

The sequential Mann–Kendall (SQMK) test [50] helps to identify breakpoints and the significance of trends in a data series  $x_i$ . This test is calculated using the ranked values  $y_i$  of the original series  $(x_1, x_2, x_3, \dots, x_n)$ . The magnitudes of  $y_i$  ( $i = 1, 2, 3, \dots, n$ ) are compared to those of  $y_j$  ( $j = 1, 2, 3, \dots, i - 1$ ). For each comparison, the cases where  $y_i > y_j$  are counted and noted as  $n_i$ . A statistic  $t_i$  is defined as follows:

$$t_i = \sum_{j=1}^i n_i$$

The distribution of the test statistic  $t_i$  has an average

$$E(t_i) = \frac{i(i-1)}{4}$$

and a variance as follows:

$$Var(t_i) = \frac{i(i-1)(2i+5)}{72}$$

The sequential values of a reduced or standardized variable, called the statistic  $u(t_i)$ , are calculated for each of the statistical variables  $t_i$  as follows:

$$u(t_i) = \frac{t_i - E(t_i)}{\sqrt{var(t_i)}}$$

The forward sequential statistic, called  $U(t_i)$ , is estimated based on the original rainfall series. The backward sequential statistic, called  $U'(t_i)$ , is calculated in the same way, but starting from the end of the original rainfall series. Abrupt changes in the rainfall series are identified by plotting  $U(t)$  and  $U'(t)$ . The point of intersection of these two curves indicates a potential location for an abrupt change. The change becomes significant at the 0.05 level when one or more points in the  $U(t)$  series exceed the significance level of  $\pm 1.96$  [51].

(B) *Pettitt test*

The Pettitt test [52] is based on the Mann–Whitney two-sample test (rank-based), and allows the detection of a single shift at an unknown time  $t$ . The null hypothesis is no change in the distribution of a sequence of random variables; the alternative hypothesis is that the distribution function  $F_1(x)$  of the random variables from  $X_1$  to  $X_t$  is different from the distribution function  $F_2(x)$  of the random variables from  $X_{t+1}$  to  $X_T$ . Let us write

$$D_{ij} = \text{sgn}(X_i - X_j) = \begin{cases} -1 \wedge (X_i - X_j) < 0 \\ 0 \wedge (X_i - X_j) = 0 \\ +1 \wedge (X_i - X_j) > 0 \end{cases}$$

where  $X_i$  and  $X_j$  are random variables with  $X_i$  following  $X_j$  in time. The test statistic  $U_{t,T}$  depends on  $D_{ij}$  as

$$U_{t,N} = \sum_{i=1}^t \sum_{j=t+1}^N D_{ij}$$

The statistic  $U_{t,N}$  is the same as the Mann–Whitney statistic for analyzing when the two samples  $X_1, \dots, X_t$  and  $X_{t+1}, \dots, X_T$  arise from the same population. The test statistic  $U_{t,N}$  is assessed for all random variables from 1 to  $N$ ; then, the most significant change point is selected where the value of  $|U_{t,N}|$  is the largest:

$$K_N = \max_{1 \leq t < N} |U_{t,N}|$$

A change point occurs at time  $t$  when the statistic  $K_N$  is significantly different from zero at a given level. The approximate significance level is given by:

$$p = 2 \cdot \exp\left(\frac{-6K_N^2}{N^2 + N^3}\right)$$

Once the  $p$ -value is less than the pre-assigned significance level  $\alpha$ , we can reject the null hypothesis and divide the data into two sub-series (before and after the location of the change point) with two different distribution functions.

### (C) *The Mann–Kendall test and Sen’s Slope*

The non-parametric Mann–Kendall test and Sen’s Slope were also applied to our data to characterize the trend, its significance, and its magnitude in the annual and seasonal series. The Mann–Kendall test [53,54] is one of the most widely used tests by researchers worldwide to determine the trend and its significance in hydrometeorological series. It is a non-parametric test, unlike linear regression; it does not assume a linear trend or normally distributed residuals. It is a robust test to outliers and extreme values. Sen’s Slope is expressed here as the rate of change over 58 years (1961–2019) in mm per year.

## 3. Results

Monitoring the relationship between drought and rainfall patterns allowed us to identify turning points. To this end, we used Pettitt’s test to demonstrate the existence of dates that saw significant changes in rainfall. The Mann–Kendall sequential test also enabled the identification of turning points in hydroclimatic series, while the classical Mann–Kendall test and Sen’s Slope test focus on exploring overall trends in the variables under study.

### 3.1. Pettitt Test

The results of the break test presented in Table 4 and Figure 2 show a sharp change in 1975–1976 for the Ait Khabbach station and in 1981–1982 for the other two stations, Dar El Hamra and Elmers. Average annual rainfall fell after the year of the break, dropping from 447 mm to 357 mm at Ait Khabbach, and from 560 mm to 459.6 mm at Dar El Hamra, representing a deficit of nearly 100 mm. The El Mers station exhibits the same trend, with a rainfall decrease of 84 mm over the study period.

**Table 4.** Pettitt test results for the hydrological year of the break point.

ID	Station	Hydrological Year of the Break Point	The Annual Rainfall (mm) and Mean Flow Before (m <sup>3</sup> /s)	The Annual Rainfall (mm) and Mean Flow After (m <sup>3</sup> /s)
S1	Ait Khabbach	1975–1976	447.22	357.56
S2	Dar El Hamra	1981–1982	560.77	459.6
S3	El Mers	1981–1982	508.03	424.37
H1	Ain Timedrine	1979–1980	21.7 m <sup>3</sup> /s	12.57 m <sup>3</sup> /s
H2	Pont Mdez	1979–1980	8 m <sup>3</sup> /s	4.96 m <sup>3</sup> /s

This decline in rainfall at mountain stations, combined with rising temperatures increases atmospheric demand through evaporation, and reduces the snowpack extent and duration. All these factors lead to a decrease in water levels in the springs and streams of this upstream area, considered the water tower of Morocco. The effect is direct on runoff; the Pettitt test applied to the two hydrological series shows a tipping point as early as 1979–1980.

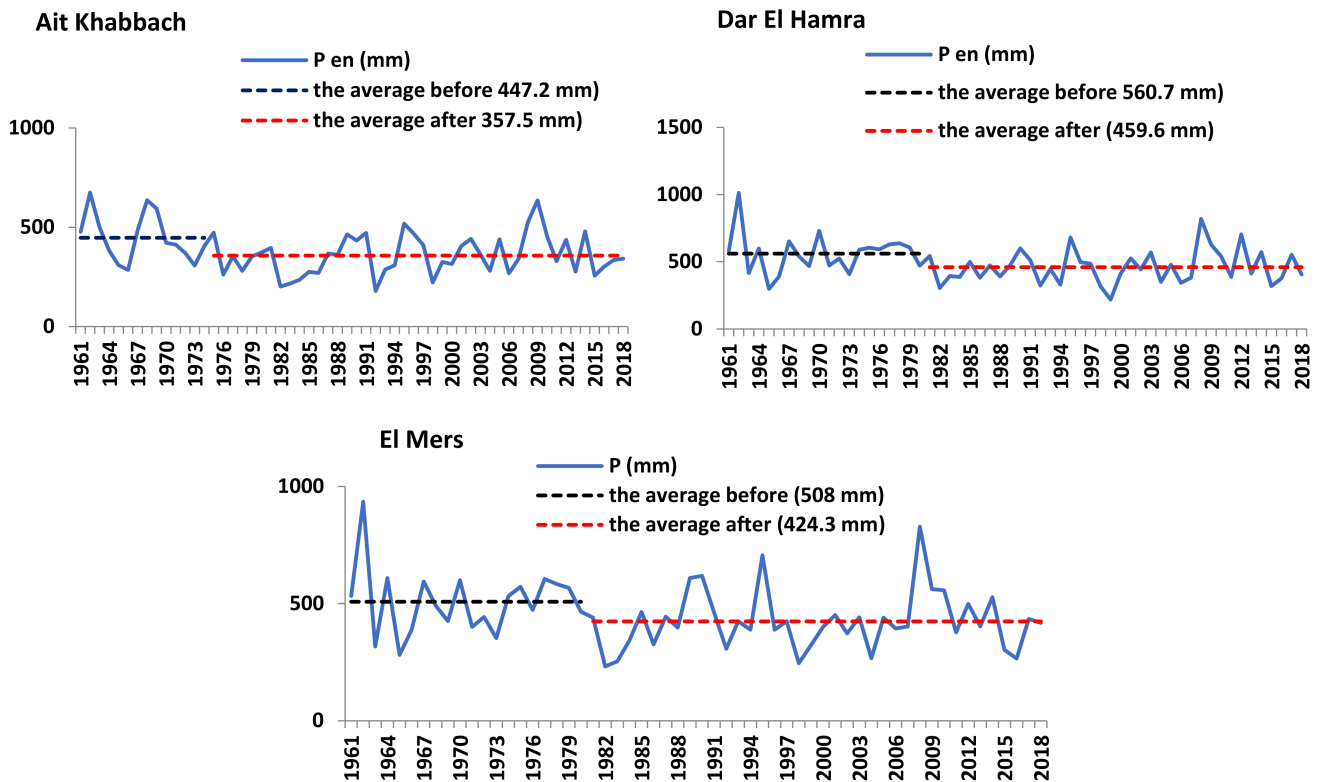


**Figure 2.** The evolution of annual rainfall at the three stations, with the average before and after the break.

### 3.2. SQMK Test of Rainfall Series

The Mann–Kendall (SQMK) sequential test illustrates points of change towards decreasing rainfall in all the hydroclimatic series used in this study. Figure 3 shows a point of change as early as 1963 for Ait Khabbach, and from 1980 for the other two rain gauge stations. For the flow series, the years 1975–1976 and 1976–1977 mark a point of decreasing flow for the Ain Timedrine and Pont Mdez stations, respectively. This is consistent with the Pettitt test. This decline only first becomes significant after 1976 for S1, 1999 for S2, and 2003 for S3, and the return of rainfall after these dates brings some of the trends below the level of significance again (Figure 3).

The Ut series curve for station H2 reached the 95% confidence limit in 1983–1984 (Pont Medz), and that of H1 (Ain Timedrine) in 1980–1981. Despite a return of rainfall in 1996 and 2009–2010, the decline in the hydrological series continued and remained significant at the 5% level until the end of the series (Figure 3). The decline in flow is not explained solely by a reduction in rainfall but also by an increase in speculative agricultural activities on the Atlas plateaus [55], which supply the flow to both measurement stations. A rise in temperature, which accentuates atmospheric demand, was also mentioned above as a contributing factor to flow decline.

### 3.3. Variability of Meteorological Drought on Annual and Seasonal Scales

The SPI12 index of the three stations, illustrated in Figure 4, shows very strong synchronisms between the stations due to their proximity. High variability in precipitation from year to year is reflected in both positive and negative SPI values.

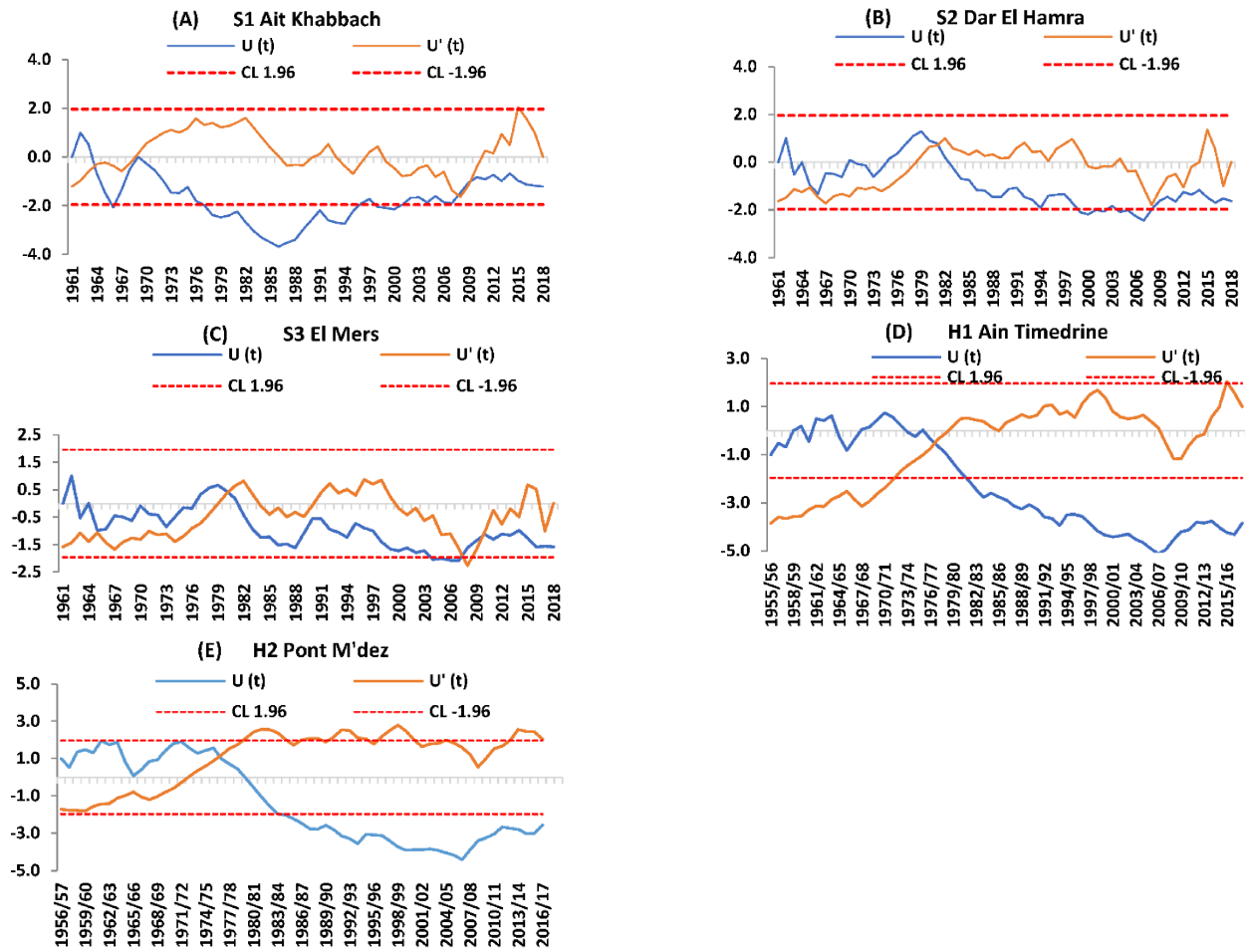


Figure 3. TSMQ for rainfall series (A–C) and hydrological series (D,E).

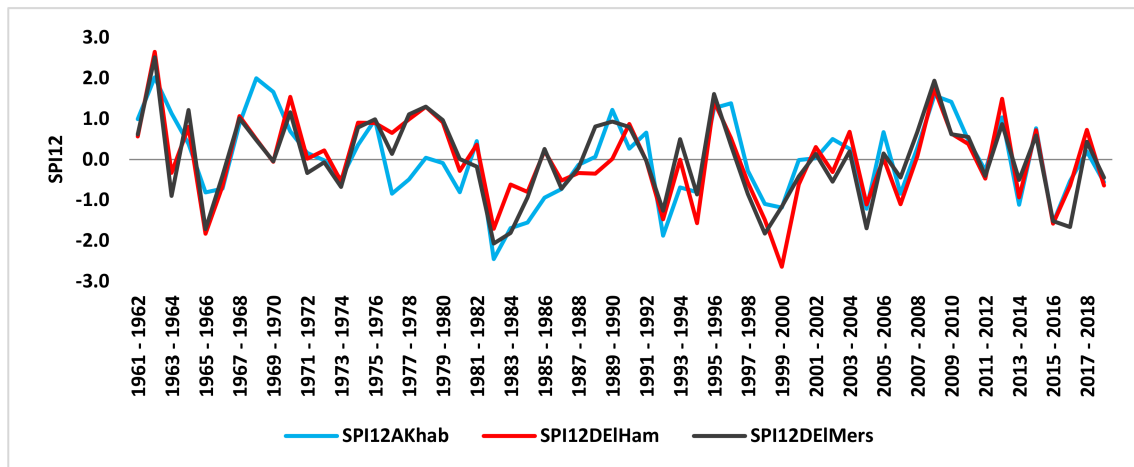


Figure 4. SPI12 from the three stations Ait Khabbach, Dar El Hamra and El Mers.

Over a 58-year study period, 28 drought events were recorded, with minimum SPI values of  $-2.45$  in Ait Khabbach,  $-2.63$  in Dar El Hamra, and  $-2.06$  in El Mers. These values were recorded during the extreme drought of 1982–1983 for Ait Khabbach and El Mers, while the Dar El Hamra station recorded its extreme value in 1999–2000.

The drought events are concentrated in the years following 1979–1980, i.e., after the previously identified tipping point or change. A succession of droughts after this date is noteworthy. Between 1980–1981 and the end of the series (39 years), 21 years had negative

SPI12 values in Ait Khabbach (54%), 23 years in Dar El Hamra (59%), and 21 years in El Mers (54%).

In terms of duration, three phases of drought characterize this period: an initial six-year drought from 1982–1983 to 1987–1988, a second wave of drought lasting three years from 1992–1993 to 1994–1995, followed by a four-year drought from 1997–1998 to 2000–2001, peaking in 1999–2000. After two very wet years in 2008–2009 and 2009–2010, a return of drought in the form of dry years separated by wet years was observed, as was the case in 2011–2012, 2013–2014, and 2015–2016, which was a very severe drought year, then 2016–2017 and 2018–2019.

At the seasonal level, our analysis focuses on the number of drought events by severity level and by station (Table 5). Over the study period, autumn and summer were the seasons most affected by meteorological drought, with 51 events distributed across the three stations. If we exclude summer, which is the normal dry season in the study area, winter and spring follow with 48 and 42 events, respectively.

**Table 5.** Number of drought events by severity level and by season in the three rain gauge stations (1961–2018).

Classes	SPI Class	Autumn			Winter		
		El Mers	Ait Khabbach	Dar El Hamra	El Mers	Ait Khabbach	Dar El Hamra
Slightly dry near normal	−0.5 to −0.99	5	5	9	9	10	2
Moderately dry	−1 to −1.49	7	5	7	6	2	11
Severely dry	−1.5 to −1.99	3	5	1	0	1	3
Extremely dry	−2 and less	1	1	2	2	2	0
<b>Total events</b>	<b>Total</b>	<b>16</b>	<b>16</b>	<b>19</b>	<b>17</b>	<b>15</b>	<b>16</b>
Evaluation	SPI class	Spring			Summer		
		El Mers	Ait Khabbach	Dar El Hamra	El Mers	Ait Khabbach	Dar El Hamra
Slightly dry near normal	−0.5 to −0.99	6	11	2	7	6	8
Moderately dry	−1 to −1.49	3	4	3	7	6	5
Severely dry	−1.5 to −1.99	0	1	0	3	1	3
Extremely dry	−2 and less	4	3	5	1	2	2
<b>Total events</b>	<b>Total</b>	<b>13</b>	<b>19</b>	<b>10</b>	<b>18</b>	<b>15</b>	<b>18</b>

At the station level and according to drought categories, and specifically during the autumn season, the Dar El Hamra station recorded 19 events, followed by the other two stations with 16 dry autumn seasons (Table 5). The majority of these events were of low or medium intensity, while there were two extreme events at Dar El Hamra and only one event each at El Mers and Ait Khabbach. Autumn droughts were concentrated in the 1970s, 1980s, and 1990s for the two stations of El Mers and Ait Khabbach, whereas the Dar El Hamra station did not exhibit homogeneous and continuous episodes of drought.

Winter saw 17 drought events recorded at El Mers, and 15 and 16 events at Ait Khabbach and Dar El Hamra, respectively. These events are concentrated in the periods 1979–1980 and 1985–1986, 1991–1992 and 1994–1995, and then from 1999–2000 to 2004–2005. The Ait Khabbach station recorded a continuous drought phase from 2010–2011 to the end of the series; this severe drought is also reflected in the El Mers series.

In spring, the Ait Khabbach station recorded 19 drought events, compared to 13 in El Mers and only 10 in Dar El Hamra (Table 5). While many of these events were of low to medium intensity (−0.5 to −1.49), the extreme drought category was strongly represented during this season, with five events in Dar El Hamra, four in El Mers, and three in Ait Khabbach. Three spring seasons recorded extreme drought values. These were recorded after the year 2000: 2004–2005, 2013–2014, and 2016–2017 for the three series studied.

This situation is explained by the decline in spring rainfall, which leads to a longer dry season and very high variability. The frequency of drought events during the wet

season (winter and spring, and partially in autumn) directly impacts the amount of water resources in this area.

### 3.4. Analysis of SDI Series Across Multiple Time Scales

The impact of this negative rainfall trend is directly reflected in the flow rates of water sources and wadis, resulting in a significant decrease in water input. The Streamflow Drought Index (SDI) is standardized similarly to the SPI and is used to identify and classify changes in the flow rates of a spring, wadi, river, etc.

On an annual time scale, Figure 2 presents two distinct phases. The first, relatively wet phase extends from the beginning of the series until 1979–1980, the year of the break revealed by the Pettitt test. This is followed by a succession of deficit years since the break recorded towards the end of the 1970s. The synchronization with annual precipitation totals is quite strong (the dotted line). Of the 38 years after 1980, 28 were deficit years (73.6%) and only 10 were surplus years; the surpluses were small and in no way compensated for the prolonged deficits.

The karst nature of the hydrological flow of the Ain Timedrine spring shows a direct response between the abundance or scarcity of rainfall and the flow recorded at the annual level, but also long-term impacts of meteorological drought. The deficit year of 1980–1981 caused the SDI to fall to negative values ( $-0.57$ ) even after a return of rain in 1981–1982 (458.60 mm) (SDI recorded  $-0.62$ ). This deficit deepened further with successive droughts until 1995–1996, an average year with rainfall totals of 542 mm and an SDI index of 1.31 (Figure 5A). A wave of drought took hold with years of deficit between 1997–1998 and 2007–2008, plunging the SDI index into negative values despite the two slightly less dry years of 2001–2002 and 2002–2003. This situation only reversed after the two wet years of 2008–2009 and 2009–2010, with a maximum drought flow value recorded in 1999–2000 of  $-2.18$ . The SDI index slowly recovered after a replenishment of underground reserves in the karst relief of the Middle Atlas to the west, south and east of this reference source. A return of droughts in 2011–2012, 2013–2014, 2014–2015, 2015–2016, and 2016–2017 plunged this index back into negative values as a direct response to the rainfall deficit in the northeastern Middle Atlas region. This rainfall deficit corresponds to a snow deficit on the peaks of Bouyblane and others, which, combined with rising temperatures and the relatively high porosity of the geological formations in this area, explains the direct and immediate response of karst spring flows to the observed rainfall deficit.

The SDI of the Pont Mdez station (Figure 5B) measures the flow of the upper Sebou River, which is currently submerged by the waters of the Mdez dam reservoir. The hydrological record of this station exhibits a hydrological behavior similar to that of the Ain Timedrine station, except for the maximum cumulative rainfall during wet years, such as 2008–2009 and 2009–2010. The upper Sebou Basin records high flow rates due to the size of its surface area, which should be compared with the hydrogeological basin of the Ain Timedrine spring, which is largely controlled by its opening at the spring site itself.

Over the period studied, from 1956–1957 to 2016–2017, two phases were observed: a wet phase before 1980 and a drier phase after that date. This was confirmed by the Pettitt test, which revealed a highly significant break ( $p < 0.001$ ) for both stations during the 1979–1980 hydrological year. Since 1980, the station has recorded 29 years (78%) with a deficit compared to only 8 years with a surplus, showing the clear dominance of drought conditions.

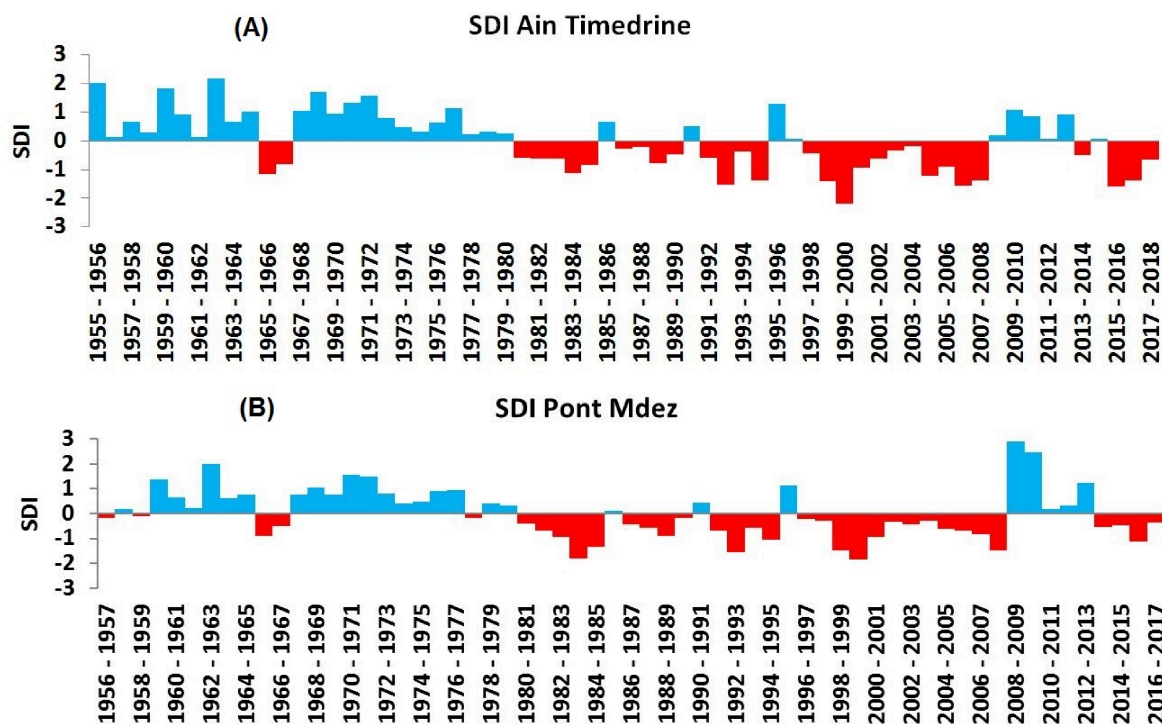


Figure 5. Annual SDI for the Ain Timedrine and Pont Mdez hydrological stations.

Regarding the seasons, Figures 6 and 7 present the SDI for the two hydrological stations. For the Pont Mdez station, the SDI recorded an extreme drought event (ED) in the autumn of the 1983–1984 hydrological year with an SDI of  $-2.14$ , followed by two severe drought seasons (SD) in 1984–1985 and 2000–2001 with SDI values of  $-1.64$  and  $-1.92$  respectively, representing 6% of the seasons in the series. Moderate drought events (MD) occurred in six seasons concentrated in the 1980s and 1990s, including 2005–06, representing 18% of the autumns in the studied series. A non-significant change point was identified in 2000–2001, indicating a return to positive flows after years of dry autumns. In winter at the same station, mild drought events predominate (69% of seasons), followed by moderate droughts (25% of seasons), concentrated in the 1980s and 1990s, followed by 2005–2006, 2006–2007, and 2015–2016. A significant change point was observed in 1978–1979, consistent with the other hydrological station at Ain Timedrine (Table 4). In spring, which is part of the wet season, the SDI at the Pont Mdez station records 70% of drought events in the mild drought category, i.e., 23 out of 61 seasons in the studied series, followed by 7 moderate drought (MD) seasons centered on the 1980s and 1990s, 2 severe drought seasons (2007–2008 and 2016–2017), and one extreme season with an SDI of  $-2.12$  in 1999–2000. A significant change point is identified in 1981–1982 with a  $p < 0.0009$ .

The Ain Timedrine station exhibits a different hydrological pattern with its groundwater reserves. In autumn, 31 events are recorded, including 20 seasons with mild drought (MD), representing 65% of the total. These are followed by 8 seasons with an average SDI between  $-1$  and  $-1.5$ , representing 26% of the autumns during the study period (1961–2018). These events are concentrated in the 1980s and 1990s, in addition to 2000–2001, 2015–2016, and 2016–2017. A significant change point was identified by the Pettitt test in 1979–1980. Severe droughts account for three out of the total, representing 10% of the total, a category that includes 2004–2005 and 2005–2006, in addition to 1984–1985. This tells us about the impact of the droughts of the 1980s and 1990s, but also of the frequent and severe droughts after 2000.

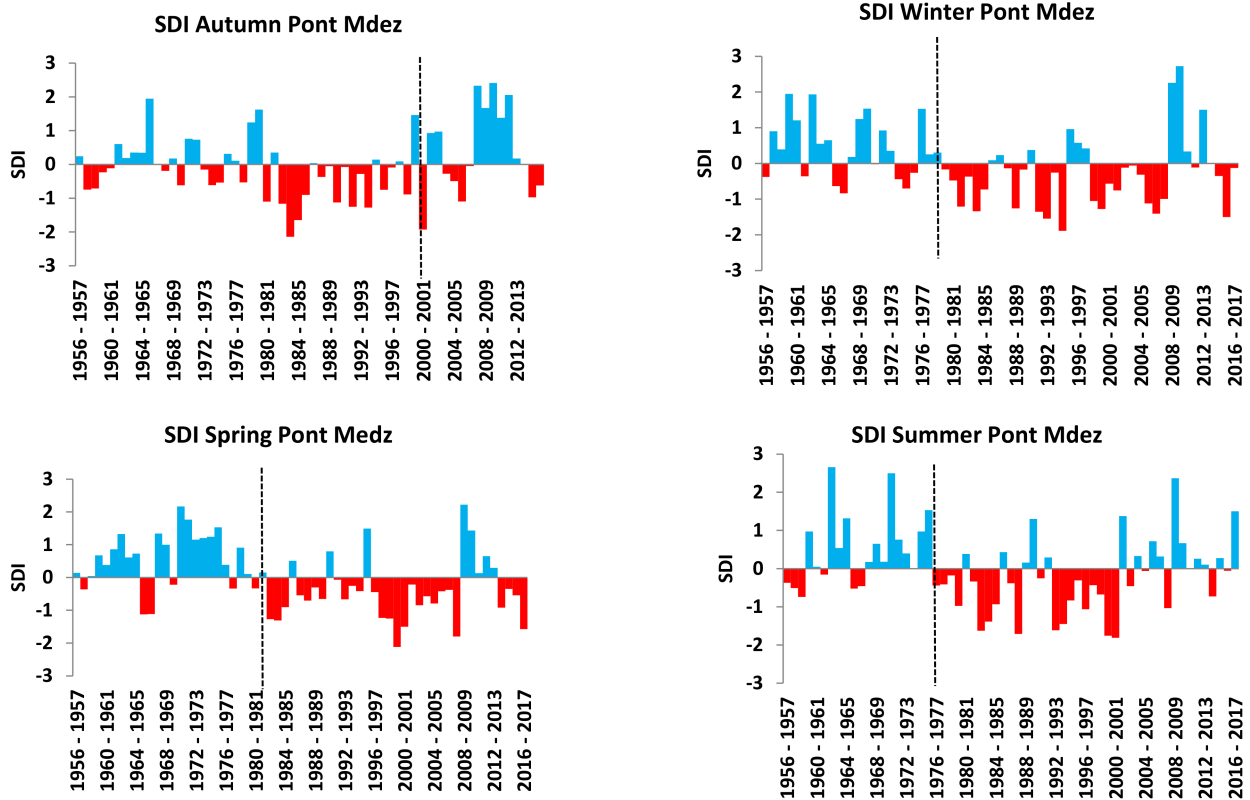


Figure 6. SDI at Pont Mdez station. The dotted line illustrates the point of change according to the Pettitt test.

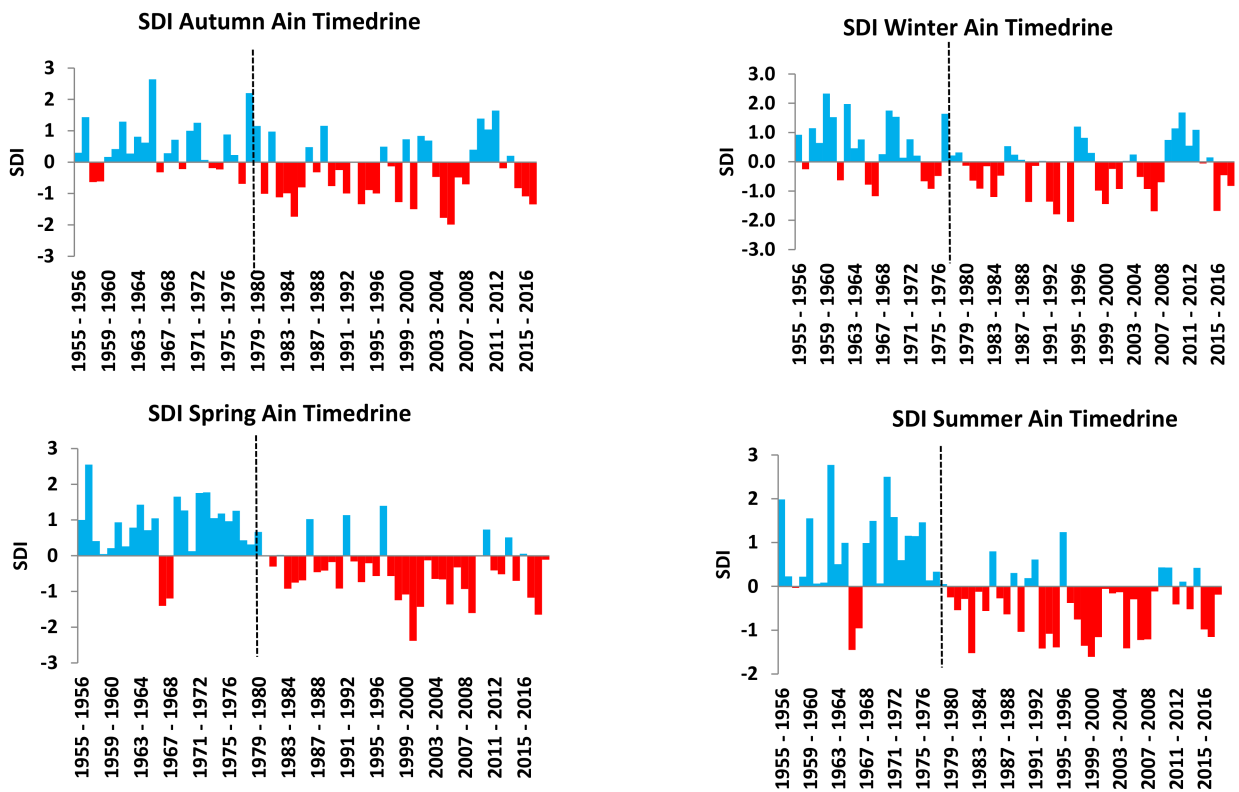


Figure 7. The SDI at the Ain Timedrine karstic spring station. The dotted line illustrates the point of change according to the Pettitt test.

In winter, the SDI recorded a significant break in 1978–1979 (Table 6), with 31 low-flow events, of which 71% were of low intensity, 16% of medium category, 10% (3 events) of severe category and one season with an extreme SDI recorded in the winter of 1994–1995 with a value of  $-2.05$  (Table 5). Figure 6 illustrates this sharp change towards deficit winter flows from the karst spring despite the few wet years such as 1995–1996 and 2009–2010, which remain exceptions in a deficit period that began in the early 1980s. In spring, a change point was identified in 1979–1980, consistent with the other seasons, especially autumn, with  $p < 0.0001$ . This illustrates the previously mentioned changes in rainfall and even snowfall on the peaks of the Middle Atlas, which constitutes the hydrological reserve of the spring in question. Summer, the season of lowest water levels, recorded a change point similar to that of winter, which is highly significant (Table 6). The regulatory role of karst springs in flow is clearly demonstrated by the change points recorded by the Ain Timdrine station, centered on the late 1970s, compared to different dates revealed by the Pont Mdez station series. This allows us to understand the difference between the two types of flow and the mechanisms that govern them (Figures 6 and 7).

**Table 6.** The point of change in the SDI series by season according to the Pettitt test.

Station	Autumn	Winter	Spring	Summer
H1 Ain Timdrine	1979–1980	1978–1979	1979–1980	1978–1979
<i>p value</i>	<b>0.01084</b>	<b>0.03629</b>	<b>0.00003386</b>	<b>0.0001113</b>
H2 Pont Mdez	2000–2001	1978–1979	1981–1982	1975–1976
<i>p value</i>	0.3265	<b>0.0325</b>	<b>0.0009088</b>	0.1061

In summary, the frequency of drought events affecting seasonal flow rates remains more pronounced at the Pont Mdez station during autumn and winter, which is normal for a watercourse that relies primarily on rainfall and surface runoff. However, in summer, the Ain Timdrine karst spring exhibits a frequency of 33% compared to 31% for Pont Mdez (Figure 8). This is unusual for a karst spring expected to regulate flow rates, but this result, although marginal, reflects the fragility of the springs and karst aquifers in this area, which are being depleted by persistent drought and the heavy pumping by speculative agricultural operations in the Middle Atlas plateaus, contributing to this decline.

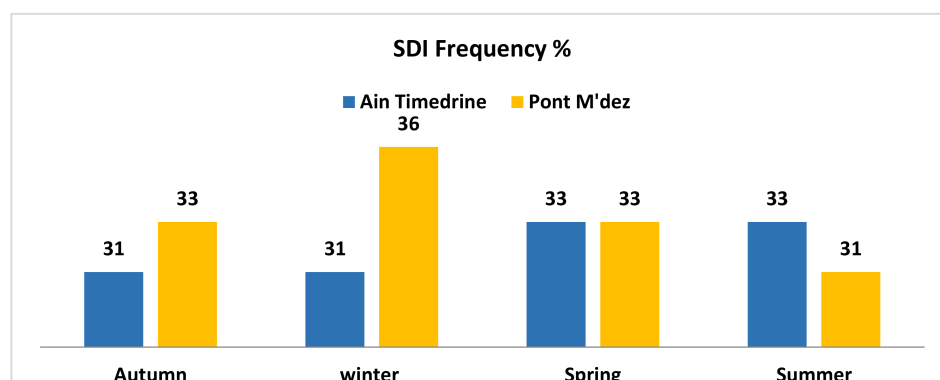


**Figure 8.** Frequency of flow drought (SDI) per season at the two hydrological stations.

At the monthly level, we opted for the SDI3 time scale to identify a break point. The Pettitt test applied to the SDI3 series from the two hydrological stations shows a break point in November 1980 for both stations Figure 9, with a fairly strong significance ( $p < 0.0001$ ). This break is repeated at other time scales, especially annual ones.

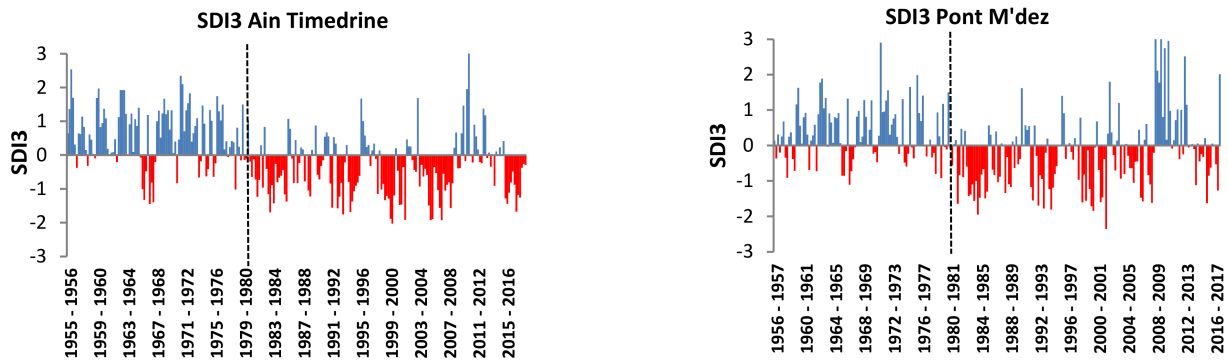


**Figure 9.** The SDI3 of the Ain Timedrine and Pont Mdez hydrological series; the dotted line illustrates the point of change according to the Pettitt test.

Figure 10 illustrates the frequency of droughts per month, still based on the SDI. Lower SDI drought frequencies than those at the Pont Mdez station are exhibited by the Ain Timedrine spring over 8 months of the year, illustrating the regulating role of karst system flow.

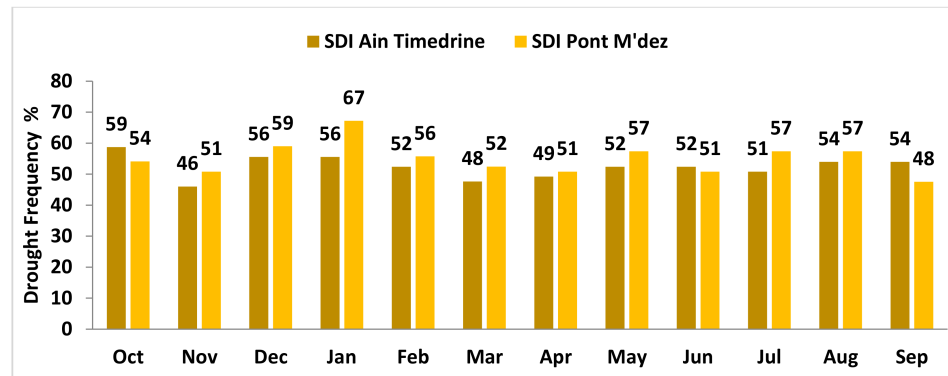


**Figure 10.** Frequency of streamflow drought (SDI) per month at the two hydrological stations.

At the Pont Mdez station, the winter months of December, January, and February recorded relatively high rates of low flow, at 59%, 67%, and 56%, respectively. This demonstrates the high variability of surface flow even during the winter season. In contrast, the highest frequency of low flow at Ain Timedrine is recorded during October, at 59% of the month, which is normal after a very long summer season that depletes the spring’s underground reserves.

*3.5. Correlation Between the SPI and SDI Indices of the Seasons*

A simple correlation between the SPI and SDI indices of the seasons was performed in order to observe the links between these variables; the threshold significance level was taken as 0.05. Figure 11 presents the result.

The SPI series from the three stations are highly and significantly correlated with each other for each season—winter, autumn, etc. The correlations between the SDI series from the two stations are also strong, both with each other and with the SPI from upstream stations. This is quite normal given the proximity of the stations, but the mechanisms controlling the climate in this area mean it is almost the same climate with very slight variations. The summer SDI at Ain Timedrine is strongly correlated with the spring SDI index at Pont Medz, as well as with the summer SPI indices of upstream stations such as El Mers and Dar El Hamra. The winter SPI at El Mers is significantly correlated with the SDI indices of the two hydrological stations.

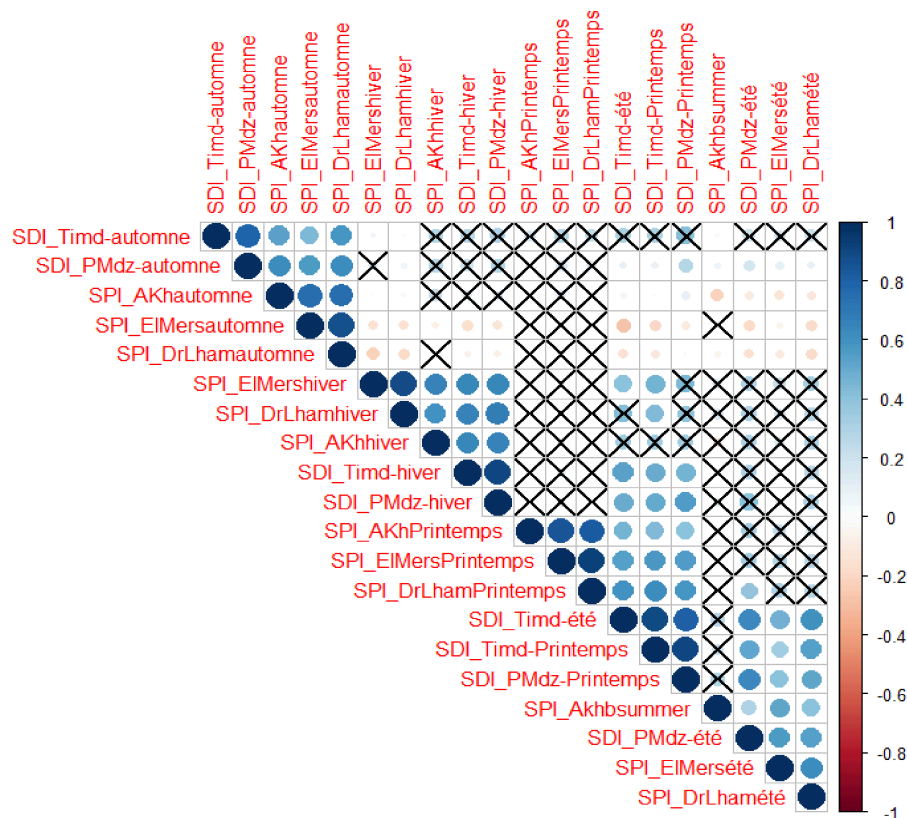


**Figure 11.** The correlation matrix between the SPI and SDI series by season in the same hydrological year of the studied stations, with significance level (squares with an X represent non-significant correlations at the 0.05 level).

Significant negative correlations were observed between the autumn and summer SPI indices at Ait Khabbach, and between the spring and summer SDI indices at Ain Timedrine and the autumn SPI at El Mers. Winter rainfall replenishes groundwater reserves for the Ain Timedrine karst spring, with a strong and significant correlation between the winter SPI indices of upstream stations and the spring SDI at Ain Timedrine.

3.6. SPI and SDI Trends by Season

Trend tests applied to the SPI series show a downward trend in SPI values during winter and spring. This decline is linked to the decrease in rainfall already mentioned above (Table 7). The winter and spring SPI series show a decrease at El Mers and Ait Khabbach, with  $p < 0.05$  at Ait Khabbach in winter and  $p < 0.1$  at El Mers in spring. The Dar El Hamra station records a significant decline in SPI values during spring and summer ( $p < 0.05$ ). The SPI calculated over a 3-month time scale shows a significant negative trend at El Mers and Dar El Hamra.

**Table 7.** Trend in the SPI values by season and SPI3 of rainfall series.

	El Mers			Ait Khabbach			Dar El Hamra		
	Z Mann–Kendall	Sen’s Slope	p Value	Z Mann–Kendall	Sen’s Slope	p Value	Z Mann–Kendall	Sen’s Slope	p Value
<b>SPI Autumn</b>	1.4800	0.0127	0.1389	0.4543	0.0027	0.650	0.7503	0.0067	0.4531
<b>SPI Winter</b>	−0.6471	−0.0060	0.5175	−2.0057	−0.0159	0.045	0.2823	0.0022	0.7778
<b>SPI Spring</b>	−1.8655	−0.0146	0.0621	−0.9156	−0.0084	0.360	−2.2373	−0.0142	0.0253
<b>SPI Summer</b>	−0.1308	−0.0011	0.8950	1.4020	0.0113	0.161	−3.5246	−0.0244	0.0004
<b>SPI3 month</b>	−1.699	−0.0003	0.089	−0.466	−0.0001	0.642	−3.664	−0.001	0.0002

An upward trend in SPI values, though not statistically significant, was observed in autumn across all three series, a finding already reported in the literature. A rise in SPI

values was also observed in Ait Khabbach during the summer. This situation was also highlighted in our previous work [56]. It illustrates a shift in the regional climate system, with a slight increase in autumn rainfall beginning as early as summer. This phenomenon affects the Moulouya region and its surrounding areas (Table 7).

The overall trend in the hydrological series is downward. The trend in the SDI series is negative in all seasons, with significant declines. The SDI of the Ain Timedrine H1 karst spring shows a strong and significant decline in autumn, spring, and summer, as does the SDI3 index. The Pont Mdez SDI index also registers a significant downward trend in spring, as does the SDI3 index (Table 8).

**Table 8.** Trend in SDI values by season and SDI3 of the two hydrological series.

	<i>(H2) Pont Mdez</i>			<i>(H1) Ain Timdrine</i>		
	Z Mann–Kendall	Sen’s Slope	p Value	Z Mann–Kendall	Sen’s Slope	p Value
<b>SDI Autumn</b>	−0.4199	−0.0036	0.6745	−2.3612	−0.0210	0.0182
<b>SDI Winter</b>	−1.6177	−0.0131	0.1057	−1.2735	−0.0103	0.2028
<b>SDI Spring</b>	−2.8155	−0.0260	0.0049	−3.9307	−0.0351	0.0001
<b>SDI Summer</b>	−0.9569	−0.0070	0.3386	−3.2148	−0.0281	0.0013
<b>SDI 3 month</b>	−5.4479	−0.0009	0.0000	−11.5710	−0.0020	0.0000

The decline in rainfall during the wet season since 1979 has depleted the underground reserves of the Ain Timedrine karst spring. Despite a return of rain in a few years, albeit with varying degrees of wetness, this has not compensated for the reduced precipitation during the peak wet season (winter and spring). This situation is compounded by an increase in irrigated agricultural activity on the Middle Atlas plateaus. All of these factors explain the negative trend in the SDI series at Ain Timedrine. The Pont Medz SDI series exhibits a different, more variable pattern that reflects surface runoff dependent on direct rainfall. An observation of Figure 9, which presents the SDI3 series from the two hydrological stations, shows a rapid response with peaks in surface runoff at Pont Medz, compared to a slower regime linked to the karst system at Ain Timedrine.

#### 4. Discussion

This work on the links between rainfall, meteorological drought, and hydrological drought in the upper Sebou region illustrates a decline in rainfall in the studied time series. This decline is manifested by droughts since 1979, which is consistent with previous work on the climate of Morocco [2]. A persistence of drought in Northwest Africa has also been found by [6,57].

The correlations between the SPI and SDI indices are very strong and synchronous, even for the karstic system, consistent with the results of [49,58] for the Oum Er Rbia basin. Winter season SPI values explain the flows of the same season, as well as the following spring and summer. In another watershed near our study area, the SDI and SRI indices are used, in addition to indices based on spatial remote sensing [59], and obtained similar results in terms of trends and exacerbation of meteorological and hydrological drought.

A recent study [60] shows a downward trend in runoff in the Mediterranean basin, between −8% and −12%. This raises further questions about the rationale behind the policy of constructing increasingly large dams, as was the case in Morocco, which is among the countries building the most dams [61]. Given the constraints of evaporation, especially in summer and in continental areas, a paradigm shift away from large dams towards smaller, even very small, dams and reservoirs is needed to enhance infiltration and groundwater recharge (water harvesting structures are increasingly being used) [62,63] and mitigate the limitations imposed by the rising atmospheric evaporative demand under a warming climate.

The high variability of rainfall in the Mediterranean climate [64], which directly influences the variability of river flows, makes it difficult to find clear trends of decreasing precipitation and streamflow time series [65]. Other studies confirmed our observed trends [66,67]. However, a slower-moving karst system has allowed us to observe and quantify this trend with stronger statistical significance, which should alert decision-makers and water resource managers in this area in particular and indeed throughout the country. The Ain Timedrine time series has made it possible to overcome the sporadic nature of wadi flows in a territory characterized by a highly variable climate and within the context of climate change.

The level of groundwater depletion is very alarming, as evidenced by the drying up of natural lakes in the Middle Atlas [55]. This necessitates urgent action to limit urban elites' access to strategic water resources in rural areas, which they can use to maintain subsistence farming and keep rural migrants in their home territories, instead of developing export-oriented agriculture of rosaceous plants and other crops that consume limited local water resources.

## 5. Conclusions

One of the aims of this article is to highlight that the groundwater resources in the Atlas Mountains, in particular, and in Morocco as a whole remain very limited and dependent on replenishment through rainfall and snowfall. We have already noted the decline observed in recent decades. Unregulated and haphazard pumping, unfortunately encouraged by public policies, is causing a decrease in the reserves of karst springs that feed the most important wadis.

Strong correlations exist between rainfall abundance and the flow rates of hydrological series. The winter SPI at upstream stations directly influences flow rates not only during winter but also throughout spring and summer. Highly porous dolomitic and limestone formations partially regulate the flow of karst springs feeding the streams. Despite this regulation, semi-arid to semi-humid climates, low rainfall, rising temperatures, and uncontrolled groundwater exploitation make karst sources vulnerable to drought-induced low flows. Detailed mapping of karst spring basins, such as Ain Timedrine, is essential to understand their extent and feeding zones. Such studies allow for better quantification and management of groundwater resources, critical for water security in increasingly hot climates.

Groundwater reserves serve as the best natural buffer in arid environments with high atmospheric demand. Rational and sustainable management of these resources is vital for rural development, particularly in Morocco and other arid/desert regions globally. The construction of the Mdez dam (since 2024) has permanently submerged the Pont Mdez station. New observation and measurement stations on other tributaries are required to accurately monitor the dam's impact and ongoing hydrological and climatic conditions.

Moroccan policies promoting cash crops for export, benefiting urban and political elites, pose a significant threat to water sustainability. A radical shift in agricultural practices is urgently needed to ensure long-term water resource sustainability. Studying climatic and hydrological drought remains critical to demonstrating the fragility of water systems. This study aims to inform public and scientific discourse and highlight unsustainable practices affecting water resources.

**Author Contributions:** Conceptualization, R.K.; methodology, R.K.; software, R.K.; validation, M.H., N.Y.K. and R.K.; formal analysis, R.K.; investigation, M.H.; resources, M.B.; data curation, R.K.; writing—original draft preparation, R.K.; writing—review and editing, N.Y.K.; visualization, R.K.; supervision, M.H. All authors have read and agreed to the published version of the manuscript.

**Funding:** This research received no external funding.

**Data Availability Statement:** The data presented in this study are available on request from the corresponding authors.

**Conflicts of Interest:** The authors declare no conflicts of interest.

## References

1. Driouech, F. Distribution des Précipitations Hivernales sur le Maroc Dans le Cadre D'un Changement Climatique: Descente D'échelle et Incertitudes. Ph.D. Thesis, L'université de Toulouse, Toulouse, France, 2010; pp. 1–164.
2. Driouech, F.; Mahé, G.; Déqué, M.; Dieulin, C.; El Heirech, T.; Milano, M.; Benabdelfadel, A.; Rouche, N. Evaluation d'impacts potentiels de changements climatiques sur l'hydrologie du bassin versant de la Moulouya au Maroc. *IAHS-AISH Publ.* **2010**, *340*, 561–567.
3. Sebbar, A.; Badri, W.; Fougrach, H.; Hsaine, M.; Saloui, A. Étude de la variabilité du régime pluviométrique au Maroc septentrional (1935–2004). *Sci. Change Planétaires/Sécheresse* **2011**, *22*, 139–148. [[CrossRef](#)]
4. Sebbar, A. Etude de la Variabilité et de L'évolution de la Pluviométrie au Maroc (1935–2005): Réactualisation de la Carte des Précipitations. PhD Thesis, Université Hassan II Mohammedia—Casablanca Faculté des Sciences Ben M'Sik, Casablanca, Morocco, 2013; p. 189.
5. Ongoma, V.; Driouech, F.; Brouziyne, Y.; Chfadi, T.; Epule Epule, T.; Tanarhte, M.; Chehbouni, A. Morocco's climate change impacts, adaptation and mitigation—A stocktake. *Reg. Environ. Change* **2024**, *24*, 14. [[CrossRef](#)]
6. Tanarhte, M.; De Vries, A.J.; Zittis, G.; Chfadi, T. Severe droughts in North Africa: A review of drivers, impacts and management. *Earth-Sci. Rev.* **2024**, *250*, 104701. [[CrossRef](#)]
7. Hssaisoune, M.; Bouchaou, L.; Sifeddine, A.; Bouimetarhan, I.; Chehbouni, A. Moroccan Groundwater Resources and Evolution with Global Climate Changes. *Geosciences* **2020**, *10*, 81. [[CrossRef](#)]
8. Analy, M.; Laftouhi, N.-E. Groundwater Depletion in an Urban Environment under Semiarid Climate and Persistent Drought—City of Marrakesh (Morocco). *Water* **2021**, *13*, 3253. [[CrossRef](#)]
9. El Bouazzaoui, I.; Lamhour, O.; Ait Brahim, Y.; Najmi, A.; Bougadir, B. Three Decades of Groundwater Drought Research: Evolution and Trends. *Water* **2024**, *16*, 743. [[CrossRef](#)]
10. Khomsi, K.; Mahe, G.; Trambly, Y.; Sinan, M.; Snoussi, M. Regional impacts of global change: Seasonal trends in extreme rainfall, run-off and temperature in two contrasting regions of Morocco. *Nat. Hazards Earth Syst. Sci.* **2016**, *16*, 1079–1090. [[CrossRef](#)]
11. Filahi, S.; Trambly, Y.; Mouhir, L.; Diaconescu, E.P. Projected changes in temperature and precipitation indices in Morocco from high-resolution regional climate models. *Int. J. Climatol.* **2017**, *37*, 4846–4863. [[CrossRef](#)]
12. Driouech, F.; Stafi, H.; Khouakhi, A.; Moutia, S.; Badi, W.; ElRhaz, K.; Chehbouni, A. Recent observed country-wide climate trends in Morocco. *Int. J. Climatol.* **2021**, *41*, E855–E874. [[CrossRef](#)]
13. Addou, R.; Obda, K.; Krakauer, N.Y.; Hanchane, M.; Kessabi, R.; El Khazzan, B.; Achir, I.E. Statistical Analysis for the Detection of Change Points and the Evaluation of Monthly Mean Temperature Trends of the Moulouya Basin (Morocco). *Adv. Meteorol.* **2024**, *2024*, 5027669. [[CrossRef](#)]
14. Noguera, I.; Vicente-Serrano, S.M.; Domínguez-Castro, F. The Rise of Atmospheric Evaporative Demand Is Increasing Flash Droughts in Spain During the Warm Season. *Geophys. Res. Lett.* **2022**, *49*, e2021GL097703. [[CrossRef](#)]
15. Verner, D.; Treguer, D.; Redwood, J.; Christensen, J.; McDonnell, R.; Elbert, C.; Konishi, Y. Climate Variability, Drought, and Drought Management in Morocco's Agricultural Sector. In *Climate Variability, Drought, and Drought Management in Morocco's Agricultural Sector*; World Bank: Washington, DC, USA, 2018. [[CrossRef](#)]
16. Schilling, J.; Freier, K.P.; Hertig, E.; Scheffran, J. Climate change, vulnerability and adaptation in North Africa with focus on Morocco. *Agric. Ecosyst. Environ.* **2012**, *156*, 12–26. [[CrossRef](#)]
17. Belmahi, M.; Hanchane, M.; El Khazzan, B.; El Mouloudi, M.; Khayati, A.; Kessabi, R.; El Kassoui, J. Assessment of the impacts of the meteorological drought on the Livestock Sector in the Province of Taza, Morocco. *Bulg. J. Agric. Sci.* **2023**, *29*, 792–799.
18. Lebdi, F.; Maki, A. *La sécheresse au Maghreb: Diagnostic, Impacts et Perspectives pour le Renforcement de la Résilience du Secteur Agricole*; Organisation des Nations Unies pour l'alimentation et l'agriculture: Tunis, Tunisia, 2023.
19. Houdret, A. The water connection: Irrigation, water grabbing and politics in southern Morocco. *Water Altern.* **2012**, *5*, 284–303.
20. Le Monde Avec AFP. Dans le Sud Marocain, des «Manifestations de la Soif» Contre Les pénuries D'eau. 2017. Available online: [https://www.lemonde.fr/afrique/article/2017/10/13/dans-le-sud-marocain-des-manifestations-de-la-soif-contre-les-penuries-d-eau\\_5200650\\_3212.html](https://www.lemonde.fr/afrique/article/2017/10/13/dans-le-sud-marocain-des-manifestations-de-la-soif-contre-les-penuries-d-eau_5200650_3212.html) (accessed on 12 October 2025).
21. Alzahid, J. Le Défi de L'eau au Maroc: Une Crise Quis' Intensifie. 2024. Available online: <https://rosaluxna.org/> (accessed on 22 October 2025).
22. Adaramola, I.; Azeez, A.; Yousufi, M.; Bibi, M.; Ali, T. Water Scarcity and Political Stability: Analyzing the Role of Water Resource Management in the Arab World. *Int. J. Sustain. Res.* **2025**, *3*, 279–298.

23. Guastello, P.; Smith, K.H.; Knutson, C.; Svoboda, M. *Drought Hotspots Around the World 2023–2025*; UNCCD Publication: Bonn, Germany, 2025.
24. Gumus, V.; El Moçayd, N.; Seker, M.; Seaid, M. Future projection of droughts in Morocco and potential impact on agriculture. *J. Environ. Manag.* **2024**, *367*, 122019. [[CrossRef](#)]
25. Kessabi, R.; Hanchane, M.; Krakauer, N.Y.; Aboubi, I.; El Kassioui, J.; El Khazzan, B. Annual, Seasonal, and Monthly Rainfall Trend Analysis through Non-Parametric Tests in the Sebou River Basin (SRB), Northern Morocco. *Climate* **2022**, *10*, 170. [[CrossRef](#)]
26. Trambly, Y.; Koutroulis, A.; Samaniego, L.; Vicente-Serrano, S.M.; Volaire, F.; Boone, A.; Le Page, M.; Llasat, M.C.; Albergel, C.; Burak, S.; et al. Challenges for drought assessment in the Mediterranean region under future climate scenarios. *Earth-Sci. Rev.* **2020**, *210*, 103348. [[CrossRef](#)]
27. Oubaha, A.; Ongoma, V.; Hssaine, B.A.; Bouchaou, L.; Chehbouni, A. Multiscale assessment of drought spatiotemporal dynamics over the Mediterranean region: A case study of Morocco. *J. Hydrol.* **2025**, *661*, 133723. [[CrossRef](#)]
28. Stamou, A.; Bakousi, A.; Dosiou, A.; Tsifodimou, Z.-E.; Karachaliou, E.; Tavantzis, I.; Stylianidis, E. Mapping Drought Incidents in the Mediterranean Region with Remote Sensing: A Step Toward Climate Adaptation. *Land* **2025**, *14*, 1564. [[CrossRef](#)]
29. Publications Office of the European Union. *Drought in the Mediterranean Region—January 2024—GDO Analytical Report*; Publications Office of the European Union: Luxembourg, 2024.
30. Fragaszy, S.R.; Jedd, T.; Wall, N.; Knutson, C.; Fraj, M.B.; Bergaoui, K.; Svoboda, M.; Hayes, M.; McDonnell, R. Drought Monitoring in the Middle East and North Africa (MENA) Region: Participatory Engagement to Inform Early Warning Systems. *Bull. Am. Meteorol. Soc.* **2020**, *101*, E1148–E1173. [[CrossRef](#)]
31. Svoboda, M.; Hayes, M.; Wood, D. Standardized Precipitation Index User Guide. *J. Appl. Meteorol.* **1987**, *63*, 197–200.
32. Hadri, A.; Ndiaye, A.S.; Khadir, L.; Jaffar, O.; Zamzami, H.A.; Mahdi El Khalki, E.; Amazirh, A.; Bouchaou, L.; Chehbouni, A. Spatio-temporal analysis of meteorological drought return periods in a Mediterranean arid region, the center of Morocco. *J. Water Clim. Change* **2024**, *15*, 4573–4595. [[CrossRef](#)]
33. Yacoub, E.; Tayfur, G. Evaluation and Assessment of Meteorological Drought by Different Methods in Trarza Region, Mauritania. *Water Resour. Manag.* **2017**, *31*, 825–845. [[CrossRef](#)]
34. Wilhite, D.A. Drought. In *Encyclopedia of World Climatology*; Oliver, J.E., Ed.; Indiana State University: Terre Haute, IN, USA, 2008; pp. 338–340.
35. Wang, W.; Ertsen, M.W.; Svoboda, M.D.; Hafeez, M. Propagation of drought: From meteorological drought to agricultural and hydrological drought. *Adv. Meteorol.* **2016**, *2016*, 6547209. [[CrossRef](#)]
36. Meskour, A.; Ahattab, J.; Aachib, M.; Hasnaoui, M.D. Assessing the impact of drought and upstream dam construction on agriculture in arid and semi-arid regions: A case study of the Middle Draa Valley, Morocco. *Environ. Monit. Assess.* **2025**, *197*, 236. [[CrossRef](#)]
37. McKee, B.T.; Doesken, J.N.; Kleist, J. The relationship of drought frequency and duration to time scales. In *Proceedings of the 8th Conference on Applied Climatology*, Anaheim, CA, USA, 17–22 January 1993; p. 6.
38. McKee, T.B.; Doesken, N.J.; Kleist, J. Drought Monitoring with Multiple Time Scales. In *Proceedings of the Ninth Conference on Applied Climatology*; American Meteorological Society: Dallas, TX, USA, 1995; pp. 233–236.
39. Vicente-Serrano, S.M.; Beguería, S.; López-Moreno, J.I. A Multiscalar Drought Index Sensitive to Global Warming: The Standardized Precipitation Evapotranspiration Index. *J. Clim.* **2010**, *23*, 1696–1718. [[CrossRef](#)]
40. Shukla, S.; Wood, A.W. Use of a standardized runoff index for characterizing hydrologic drought. *Geophys. Res. Lett.* **2008**, *35*, L02405. [[CrossRef](#)]
41. Nalbantis, I.; Tsakiris, G. Assessment of hydrological drought revisited. *Water Resour. Manag.* **2009**, *23*, 881–897. [[CrossRef](#)]
42. Tigkas, D.; Vangelis, H.; Tsakiris, G. DrinC: A software for drought analysis based on drought indices. *Earth Sci. Inform.* **2015**, *8*, 697–709. [[CrossRef](#)]
43. Tabari, H.; Nikbakht, J.; Hosseinzadeh Talaei, P. Hydrological Drought Assessment in Northwestern Iran Based on Streamflow Drought Index (SDI). *Water Resour. Manag.* **2013**, *27*, 137–151. [[CrossRef](#)]
44. Tareke, K.A.; Awoke, A.G. Hydrological Drought Analysis using Streamflow Drought Index (SDI) in Ethiopia. *Adv. Meteorol.* **2022**, *2022*, 7067951. [[CrossRef](#)]
45. Yuçe, M.I.; Deger, I.H.; Esit, M. Hydrological drought analysis of Yeşilirmak Basin of Turkey by streamflow drought index (SDI) and innovative trend analysis (ITA). *Theor. Appl. Climatol.* **2023**, *153*, 1439–1462. [[CrossRef](#)]
46. Boudad, B.; Sahbi, H.; Manssouri, I. Analysis of meteorological and hydrological drought based in SPI and SDI index in the Inaouen Basin (Northern Morocco). *J. Mater. Environ. Sci.* **2018**, *9*, 219–227. [[CrossRef](#)]
47. Zkhir, W.; Trambly, Y.; Hanich, L.; Jarlan, L.; Ruelland, D. Spatiotemporal characterization of current and future droughts in the High Atlas basins (Morocco). *Theor. Appl. Climatol.* **2019**, *135*, 593–605. [[CrossRef](#)]
48. Ben Salem, S.; Ben Salem, A.; Karmaoui, A.; Yacoubi Khebiz, M. Vulnerability of Water Resources to Drought Risk in Southeastern Morocco: Case Study of Ziz Basin. *Water* **2023**, *15*, 4085. [[CrossRef](#)]

49. Houmma, I.H.; Hadri, A.; Boudhar, A.; Karaoui, I.; Oussaoui, S.; El Khalki, E.M.; Chehbouni, A.; Kinnard, C. Analysis of the Propagation Characteristics of Meteorological Drought to Hydrological Drought and Their Joint Effects on Low-Flow Drought Variability in the Oum Er Rbia Watershed, Morocco. *Remote Sens.* **2025**, *17*, 281. [[CrossRef](#)]
50. Sneyers, R. *On the Statistical Analysis of Series of Observations*; World Meteorological Organization (WMO): Geneva, Switzerland, 1990.
51. Hanchane, M.; Addou, R. Aspects d'adaptation aux changements climatiques en milieu aride: Cas de l'Oued Melloulou (Maroc Nord Oriental). *Espac. Rev. Géographie* **2019**, N° 6–7, 63–72.
52. Pettitt, A.N. A non-parametric approach to the change-point problem. *J. R. Stat. Soc. Ser. C (Appl. Stat.)* **1979**, *28*, 126–135. [[CrossRef](#)]
53. Mann, H.B. Nonparametric Tests Against Trend. *Econometrica* **1945**, *13*, 245–259. [[CrossRef](#)]
54. Kendall, M.G.; Stuart, A. *The Advanced Theory of Statistics*; Macmillan: New York, NY, USA, 1977; Volume 1, p. 168.
55. El-Bouhali, A.; Amyay, M.; El Ouazani Ech-Chahdi, K. Changes in water surface area of the Middle Atlas-Morocco lakes: A response to climate and human effects. *Int. J. Eng. Geosci.* **2024**, *9*, 221–232. [[CrossRef](#)]
56. Kessabi, R.; Hanchane, M.; Caloiero, T.; Pellicone, G.; Addou, R.; Krakauer, N.Y. Analyzing Spatial Trends of Precipitation Using Gridded Data in the Fez-Meknes Region, Morocco. *Hydrology* **2023**, *10*, 37. [[CrossRef](#)]
57. Moutia, S. Sécheresse au Maroc dans le Contexte des Changements Climatiques: Caractérisation Spatio-Temporelle. Ph.D. Thesis, Ecole Hassania des Travaux Publics, Casablanca, Morocco, 2025.
58. Ouelkabar, F.E.; Ait Lamqadem, A.; Saafadi, L.; Pradhan, B.; Wang, G.; Ghazi, B.; Charef, K.; Laabdi, Y. Integrated drought assessment in Morocco: A combined approach using meteorological, hydrological, and remote sensing observations (1975–2023). *Model. Earth Syst. Environ.* **2026**, *12*, 172. [[CrossRef](#)]
59. Mliyah, M.M.; Aqnouy, M.; Laaraj, M.; Bouizrou, I.; Tariq, A.; Benaabidate, L.; Kraiem, H.; Shitu, K. Assessing drought dynamics in a semi-arid basin: A multi-index approach using hydrological and remote-sensing indicators. *Environ. Sci. Eur.* **2025**, *37*, 180. [[CrossRef](#)]
60. Gudmundsson, L.; Brunner, M.I.; Döll, P.; Fluet-Chouinard, E.; Frolova, N.; Gosling, S.N.; Hirabayashi, Y.; Kireeva, M.B.; Liu, X.; Müller Schmied, H.; et al. Past and future change in global river flows. *Nat. Rev. Earth Environ.* **2026**, *7*, 7–23. [[CrossRef](#)]
61. Aminzadeh, M.; Narayanaswamy, S.; Nevermann, H.; Zampieri, M.; Hoteit, I.; D'Odorico, P.; AghaKouchak, A.; Madani, K.; Shokri, N. Water storage paradox of reservoir expansion and evaporative losses in the MENA region. *Sci. Rep.* **2025**, *15*, 34297. [[CrossRef](#)]
62. Moumane, A.; Elmotawakkil, A.; Hasan, M.M.; Kranjčić, N.; Batchi, M.; Karkouri, J.A.; Durin, B.; Gomaa, E.; El-Nagdy, K.A.; Youssef, Y.M. Integrating GIS, Remote Sensing, and Machine Learning to Optimize Sustainable Groundwater Recharge in Arid Mediterranean Landscapes: A Case Study from the Middle Draa Valley, Morocco. *Water* **2025**, *17*, 2336. [[CrossRef](#)]
63. Amiri, M.; Zohair, Q.; Abdelghani, Q.; Salem, A. Integrated GIS-based multi-criteria approach for rainwater harvesting site selection in the Moulouya Basin, Morocco. *J. Hydrol. Reg. Stud.* **2026**, *64*, 103123. [[CrossRef](#)]
64. Lionello, P.; Abrantes, F.; Congedi, L.; Dulac, F.; Gacic, M.; Gomis, D.; Goodess, C.; Hoff, H.; Kutiel, H.; Luterbacher, J.; et al. Introduction: Mediterranean Climate—Background Information. In *The Climate of the Mediterranean Region*; Lionello, P., Ed.; Elsevier Inc.: Amsterdam, The Netherlands, 2012; pp. xxxv–xc. ISBN 9780124160422.
65. Vicente-Serrano, S.M.; Trambly, Y.; Reig, F.; González-Hidalgo, J.C.; Beguería, S.; Brunetti, M.; Kalin, K.C.; Patalen, L.; Kržič, A.; Lionello, P.; et al. High temporal variability not trend dominates Mediterranean precipitation. *Nature* **2025**, *639*, 658–666. [[CrossRef](#)] [[PubMed](#)]
66. Philandras, C.M.; Nastos, P.T.; Kapsomenakis, J.; Douvis, K.C.; Tselioudis, G.; Zerefos, C.S. Long term precipitation trends and variability within the Mediterranean region. *Nat. Hazards Earth Syst. Sci.* **2011**, *11*, 3235–3250. [[CrossRef](#)]
67. Deitch, M.J.; Sapundjieff, M.J.; Feirer, S.T. Characterizing Precipitation Variability and Trends in the World's Mediterranean-Climatic Areas. *Water* **2017**, *9*, 259. [[CrossRef](#)]

**Disclaimer/Publisher's Note:** The statements, opinions and data contained in all publications are solely those of the individual author(s) and contributor(s) and not of MDPI and/or the editor(s). MDPI and/or the editor(s) disclaim responsibility for any injury to people or property resulting from any ideas, methods, instructions or products referred to in the content.